January 27, 1995 Draft

Effect of an airplane cabin water spray system (CWSS) on human thermal behavior: A theoretical study using a 25-node model of thermoregulation.

by

Matthew B. Wolf and Robert P. Garner

Department of Physiology, University of South Carolina School of Medicine

Columbia, SC 29208

and

Aviation Physiology Laboratory,

The Federal Aviation Administration, Mike Moroney Aeronautical Center

Oklahoma City, OK 73125

Running head: Model of water-wetted human thermal behavior

ABSTRACT

A mathematical model was developed that could adequately describe experimentally determined transient changes in metabolic rate (MR), and core and skin temperatures of human beings exposed to water-immersion conditions (0 to 28°C). The model was the basic 25-node description of Stolwijk and Hardy, as modified to apply to a male with medium fat content. The MR increase induced by shivering was described by 3 components sensitive to 1) time-rate of change of skin temperature, 2) the product of changes in skin and head-core temperatures and 3) the product of skin temperature change and the time-rate of change of head-core temperature. The model was also able to closely predict the changes in MR and skin temperatures induced by exposure to cold air. However, the predictions of rectal temperature changes were in the opposite direction to the experimental data for this case. The model was modified to describe the effects of spraying an individual with water on their head, arms and torso to simulate the action of a cabin water spray system (CWSS) activated by a fire in an airplane. The model predicted that an individual, after being sprayed and exiting into a cold and windy enviroment, would encounter only a minor increase in thermal stress, compared to the dry state. We conclude that mathematical simulation is an effective method of predicting thermal behavior of humans under a variety of cold conditions.

Key words: Mathematical model, human thermoregulation, water immersion

INTRODUCTION

The advent of manned space flight in the 1960s spurred the development of mathematical models of human temperature regulation aimed at understanding the response to the thermal challenge of strenuous exercise in harsh environments. In the early 1960s, Wissler (20) developed an extremely complex model in which the body was subdivided into 250 tissue regions (each region lumped and considered as a node). In 1966, Stolwijk and Hardy (15) developed a much simpler 8-node model, which was expanded to 14 nodes by Kuznetz (10) in 1968 and to 25 nodes in 1971 by Stolwijk and Hardy (16). The 25-node model has become the standard anatomical approach to modelling human temperature regulation. Adoption of the Stolwijk and Hardy approach by the National Aeronautics and Space Administration (NASA) has probably contributed to the relatively widespread acceptance of the Stowijk and Hardy model.

The approach of the present study was to use the 25-node model (16) to study the effect of a cabin water spray system (CWSS) on thermoregulatory responses of passengers after being wetted by the spray system. The aim was to see if an individual, after being sprayed with water in an airplane, might be subjected to injurious thermal stresses after exiting into a cold environment. Examination of the literature revealed experimental and theoretical studies where minimally clothed humans were immersed in cold water or exposed to cold air (8,14), but no studies were found pertinent to the clothed individual being wetted and then exposed to a cold environment. Theoretically, if the 25-node model could predict human thermal changes during cold-water immersion, then it could be modified for use under water-spray conditions.

In 1972, Hardy (5) found that the controller equations of the 25-node temperature regulation model could not accurately predict the effects of cold environments on human thermal responses. As a result, in 1976, Gordon, et al. (4) developed a new model increasing the number of nodes to 42, substantially changing the form of the controller equations. This model was able to closely predict transient skin and rectal temperature changes and the increases in metabolic rate (MR) due to cold-air exposure. However, more recently, Wissler (22) found that this model was unsuitable for predicting cold-water immersion data.

The latest model of human thermoregulation was by Tikuisis et al. (17). The model was designed specifically to predict transient rectal temperature and MR data measured in that study under cold-immersion at 20 and 28°C water temperatures. They used the 25-node model, but updated the anatomical parameter values for the body composition of their experimental subjects according to the formulas given in Montgomery (11). Montgomery had expanded the 25-node model to 61 nodes to study the thermal behavior of divers in wet suits exposed to cold water, but he had kept the original cold controller equations. Tikuisis et al. (17) showed that these controller equations were inadequate to predict their data. Therefore, they modified these equations so that the shivering-induced MR increase was sensitive to the change in skin temperature, in addition to the sensitivity to the product of changes in skin and core temperature, as in the original Stolwijk and Hardy models (15,16). However, Tikuisis et al. never compared their model predictions to available data from Hayward et al. (7,8) for lower water temperatures. These data show an initial rapid rise in MR that the Tikuisis et al. model cannot reproduce. This finding led us to investigate

other possible controller formulations.

In 1985, Wissler (23) proposed a major modification of the temperature controller for the induced MR increase due to shivering. He suggested that the MR controller be composed of 3 components, the first sensitive to the rate of skin cooling, the second sensitive to some function of changes in skin and core temperatures, and the third sensitive to the rate of core cooling. There have been proponents of these individual factors in the control of shivering, but no one had proposed that all 3 were important.

In the present study, our approach was to use the 25-node model and see if a set of controller equations similar to those proposed by Wissler (23) for shivering would be sufficient to predict temperature and MR data for cold-water immersion. Our finding was that, in general, the shivering controller equations suggested by Wissler had the ability to fulfill this task. Therefore, this paper will describe 1) the details of the basic model, 2) the comparison of model prediction with literature data and 3) the modification of the model for application to the water-spray problem and the model predictions for this situation.

METHODS

The anatomical model used is essentially the 25-node model of Tikuisis et al. (18), which is derived from the original Stolwijk and Hardy model (16). Tikuisis et al (18) derived new parameter values to fit the body composition of their experimental group. Briefly, the body is subdivided into 6 parts: head, trunk, arms, legs, feet and hands. Each of these sections is further subdivided radially from the center into the concentric annular sections, core, muscle, fat, and skin. Including the blood volume, there are 25 individual anatomical units, which are assumed homogeneous and are therefore called compartments. There is a characteristic compartmental (nodal) temperature.

Heat flows radially via conduction between adjacent compartments, and heat is convected between each compartment and the central blood pool. This latter process can be modulated by vasodilation for both muscle and skin blood flows and by vasoconstriction for skin blood flows. Countercurrent heat exchange in the skin was not included. Heat transfer between the skin and the environment occurs by evaporation (insensible and sweating), conduction, convection, and radiation. Heat is produced metabolically in each compartment, except the blood. Heat production can be increased in the cold by shivering. Heat is also lost by respiration. The passive heat transfer equations for this system are those given by Stolwijk and Hardy (15).

The model anatomical parameters were for a moderate-fat content male, as described by Tikuisis et al. (18). These parameters are weight = 79.2 kg, body fat = 17.62 kg and surface area = 1.94 m^2. The parameters used for thermal conductances, capacitances, etc. are given in Tikuisis et al. (18).

Thermoregulatory control is via a central integrator, which receives information on skin and hypothalamic (head core) temperatures. This information is in the form of error signals, which indicate differences between the individual temperatures and their set-point values. Set-point values are determined from the solution of the steady-state heat transfer equations for the unclothed mathematical model under thermoneutral conditions (ambient air temperature of 28.5°C). These values are unchanged throughout the simulation process. Cold error signals from each skin section are weighted by the fraction of total skin thermoreceptors in that section (16) and summed to produce the integrated peripheral *COLDS* signal.

Efferent outputs from the central controller in response to the cold stress produce skin vasoconstriction and muscle vasodilation and metabolic heat generation through shivering. The skin vasoconstriction is driven by a linear combination of the *COLDS* signal and the hypothalamic temperature error, as used previously (16). Muscle vasodilation is proportional to the metabolic heat generation. What different in the present model is the treatment of the shivering phenomena. In 1985, Wissler (23) proposed that metabolic heat generation due to shivering could be described as the sum of 3 components, as described below. Wissler presented the general equations for these components, but did not give parameter values, even though he apparently came up with these values to compare his model predictions to experimental data.

In the present model, the shivering phenomena was modelled as follows:

$$S_1 = - A_{s1} \sum \frac{dT_{s,i}}{dt} \times SKINR\,[i] \qquad (1)$$

where S_1 is the first MR component of shivering, $dT_{s,i}/dt$ is the time rate-of-change of the ith skin temperature, $SKINR[i]$ is the fraction of skin thermoreceptors in the ith skin section and A_{s1} is a constant.

$$S_2 = - A_{s2} \times COLDS \times \Delta T_h \qquad (2)$$

where S_2 is the second MR component of shivering, ΔT_h is the change in hypothalamic temperature from the set point and A_{s2} is a constant.

$$\frac{dS_3}{dt} = K_{s3} \left(- A_{s3} \times \frac{dT_h}{dt} \times COLDS - S_3\right) \qquad (3)$$

where S_3 is the third MR component of shivering, dT_h/dt is the time rate-of-change of hypothalamic temperature, K_{s3} is a time constant, and A_{s3} is a constant. The constants for the S_1 and S_2 components were determined, as described in the RESULTS section. The constants for the S_3 component were determined from the data shown in Tables 1 and 2, which were derived from the data of Nadel and Horvath (12).

In the present study, the product effect of changes in skin and core temperatures was incorporated as the S_2 component (see Eq. 2), but the changes were derived from the thermoneutral setpoint established prior to immersion. The effect of a time lag for this component, as produced by the differential equation formulation of Wissler (23), was not included because of a lack of experimental evidence for its necessity. The S_3 component was described (see Eq. 3) as a product of skin temperature change and the rate of change of core temperature. This component was described by a differential equation because Nadel and Horvath (12) found that after the peak MR was reached, the MR subsequently declined with time back to the steady-state values. The peak values and the steady-state values were used (see Tables 1 and 2) to derive the parameter values for this relationship. The parameter values for the other constants (see Table 3) were derived to fit the model to experimental data described in the RESULTS section.

An unusual feature in the present model was a limit on the S_2 component, which varied with time (see Figure 2). This kind of limit was necessary for the model prediction to approximate the slower rise in MR after the initial peak. This limit became a factor only in the lower-temperature water immersion cases. Wissler (23) suggested that the S_2 component in his model be modified by a time-varying factor to account for MR increases during prolonged exposure to cold. He suggested that this effect could account for the influence other thermoreceptors than those in the hypothalamus and skin. Our variable limit accomplishes the same purpose and may represent the same phenomena. Alternatively, the time-varying limit may represent an increase in thermoreceptor sensitivity after prolonged intense stimulation.

This study has demonstrated for the first time that the thermal behavior of immersed humans can be predicted for a wide range of temperatures. However, it would be desirable if the model could also be applicable to cold-air exposure conditions, since no available models have been able to predict thermal behavior for both kinds of conditions. Besides the application of the model of Gordon et al. (4), which was limited to a comparison with 1 data set, Haslam and Parsons (6) recently compared rectal and skin temperature predictions of 2 different models under cold-air exposure conditions. The models were a 2-node model of Gagge et al. (2) and the 25 node Stolwijk and Hardy (16) model. They found that neither of these models could describe the data with sufficient accuracy over the entire range of cold temperatures considered. The results of the present study have shown that the model can predict changes in MR and skin temperatures for the 1 case of cold-air exposure considered (see Figures 7-9), but the rectal (core) temperature predictions are in the opposite direction to experimental findings (4). This reasons for this discrepancy have not been reconciled. Timbal et al. (19) found that the changes in MR after the initial peak occurring during water immersion of temperatures down to 24°C could be described as a function of the sum of 2 factors, 1 proportional to the change in skin temperature and the second proportional to rectal temperature. However, in their study, rectal temperature increased during the immersion, which is opposite to the findings of Tikuisis et al. (17) and Hayward et al. (7,8). Timbal et al. proposed that a decrease in skin temperature and an increase in rectal temperature both acted to increase MR. However, this relationship did not hold for cold-air exposure, so they were forced to assume a different relationship here that did not contain the influence of core temperature. Timbal et al. (19) were bothered by the conclusion that the body responds differently to the type of thermal stress, but they were left with no alternative. The

This formulation has 5 significant differences from that of Wissler (23). 1) Wissler proposed that all 3 components were time varying, since he wrote each one as a differential equation. However, he did not offer any experimental evidence for this assumption with regards to the S_1 and S_2 components. In the absence of such data, we chose the simpler formulation shown above. 2) Wissler suggested that the steady-state S_2 component has the form suggested by Hayward et al. (8). However, the data used by Hayward et al. to derive their relationship did not take into account the effect of changes in core temperature on metabolic rate, as expressed in the S_3 component. As a consequence, we incorporated only the product relationship of central and peripheral effects as in the Hayward et al. relationship. 3) Wissler proposed that the S_3 term be proportional to dT_h / dt, but did not include the modifying effect of changes in skin temperature as in our formulation. This latter effect was suggested by the experimental data of Nadel and Horvath (12), who found that the magnitude of the metabolic response to a centrally imposed heat debt depended upon the skin temperature. 4) We found it necessary to limit each of these components to some maximum value (see RESULTS). 5) Wissler multiplied the S_2 component by a time-varying factor, which accounted for the finding that metabolic rate continued to increase during prolonged exposure to cold, even though rectal and skin temperatures were relatively stable. As described below, we found it necessary to impose a limit on the S_2 term, which varied with time. Therefore, our approach may produce a similar effect as the factor used by Wissler.

The total shivering MR, *CHILL*, was then

$$CHILL = S_1 + S_2 + S_3 \qquad (4)$$

and this sum was also limited.

Simulation of head-out, cold-water immersion.

When the model was to be used to describe thermal regulation during water immersion, except for the head-skin compartment, all other skin compartments no longer transferred heat to the ambient air. Instead, they now communicated with a water layer of constant temperature. The experimental data of Hayward et al. (7,8) showed that skin temperature rapidly decreased after the immersion. We found that the same transient decreases in skin temperature could be achieved (see Fig. 3) by multiplying the skin-air heat transfer coefficients by a factor of 14 to convert them to skin-water coefficients. This procedure avoided the much more complicated approach of Tikuisis et al. (17) that required estimation of actual heat transfer coefficients.

The water temperatures considered were 28°C and 20°C to compare to the data of Tikuisis et al. (17) and 10°C and 0°C to compare to the data of Hayward et al. (7,8). Our general approach was to determine the value of the *CHILL* controller constants that gave the best overall fit to the metabolic rate and rectal temperature data from these sources.

Simulation of cabin water-spray system responses.

Our approach to simulating the effect of the CWSS on human thermoregulation was to assume that the spray produces a film of water on the unclothed skin (head) of a uniform thickness. The spray, which contacts the clothing on other parts of the body, wets this clothing and causes it to "stick" to the skin, also producing a uniform water layer, but thicker than for the unclothed surface. When the individual exits the airplane and is exposed to the ambient air, water evaporates from the layer on the head and from that in the clothing, and the thickness of these layers decreases. When the layer on any skin surface is fully evaporated, heat transfer from the skin reverts to the normal condition. In the model, heat loss (Kcal/hr) from the water layer due to evaporation is proportional to the difference between the vapor pressures of the water layer and ambient air multiplied by the convective heat-transfer coefficient between water and air (16). The rate of evaporation of the layer is this rate of heat loss divided by 0.586 cal/g (3).

Heat transfer between the skin and the water layer is by conduction. The thermal conductivity (TC_{sw}) between the skin and the water layer of varying thickness is determined at each instant in time using the approach of Tikuisis et al. (18) derived from elementary heat-transfer theory (9) as follows:

Head (sphere)

$$r_w = \sqrt[3]{(r_s^3 + \frac{3V_w}{4\pi})} \qquad (5)$$

where r_w and r_s are the outer radii of the water layer and skin, respectively and V_w is the volume of the water layer.

$$TC_{sw} = \frac{4\pi}{\frac{1}{K_s}(\frac{1}{r_{s,cm}} - \frac{1}{r_s}) + \frac{1}{K_w}(\frac{1}{r_s} - \frac{1}{r_{w,cm}})} \qquad (6)$$

where K_s and K_w are the specific thermal conductivities of skin and water, respectively, and $r_{s,cm}$ and $r_{w,cm}$ are the radii to the centers of mass of skin and water, respectively.

Trunk and arms (cylinders)

$$r_w = \sqrt{(r_s^2 + \frac{V_w}{\pi L})} \qquad (7)$$

where L is the length of the section.

$$TC_{sw} = \frac{2\pi L}{\frac{1}{K_s} \ln\left(\frac{r_s}{r_{s,cm}}\right) + \frac{1}{K_w} \ln\left(\frac{r_{w,cm}}{r_s}\right)} \qquad (8)$$

Because the water layer is relatively thin, $r_{w,cm}$ was determined as $(r_s + r_w)/2$.

When only part of a skin segment was initially in contact with a water layer, then the skin compartment was subdivided into 2 parts: wet and dry. The wet-skin compartment was in contact with its water layer, and heat transfer occurred between them. The dry-skin compartment continued to communicate with the ambient air. Each compartment communicated separately with that portion of the fat layer beneath it. Similarly, the metabolism, insensible heat loss, and blood flow were partitioned between these skin compartments on the basis of the initial fraction of skin wetted. There was no heat transfer between the wet- and dry-skin compartments. The skin temperature for a partially wet segment was the average of the wet and dry temperatures, as weighted by the fraction of thermoreceptors in each section.

The thermal effects of clothing were accounted for in the model by multiplying the heat transfer coefficient between skin and air by a constant (F_{cl}) for each body segment other than the head. F_{cl} takes on values from 0 (perfect insulation) to 1 (no insulation) as described by Gagge and Nishi (3). For the present study, F_{cl} was assumed to be 0.52, which represents a lightly clothed individual. With this clothing factor, the thermoneutral ambient temperature became 24.1°C.

The effect of wind velocity was included in the model by modifying the convective heat-transfer coefficient for each anatomical segment. The values given by Tikuisis et al. are for a standard velocity of 0.1 m/sec (0.223 MPH). It was assumed that the coefficient changes as the square root of the ratio between the ambient velocity and the standard value (16).

The initial thickness of the water layer on the thorax and arms was taken as 0.06 cm. This value gave a water-layer mass of 344 g on the thorax and 196 g on the arms if both of these area were fully wetted. The total water mass of 540 g was equivalent to the water content of a thoroughly wet, long-sleeve cotton shirt. The initial water layer on the head was assumed to be only one-half as thick (0.03 cm) because it was not covered by a layer of clothing, which would hold water and increase the effective thickness.

From design considerations of the CWSS, it was decided that a maximum of 25% of the body surface could be wetted. The first 7% wetted would be the head, and between 7% and 25%, equal surface areas would be wetted on both the thorax and arms. Therefore, for example, if 5% were wetted, then 5/7 of the head area would be wetted, and nothing on the trunk and arms. If 25% were wetted, the head would be 100% wet, whereas only 30% and 53% of the trunk and arm surface areas, respectively, would be wetted because of the larger surface area of the trunk. Under the 25% wetted condition, the initial masses of water on the head, trunk and arms were 40

g, 104 g, and 104 g, respectively.

Simulation methods

The model equations were simulated using the SCoP computer program developed at Duke University under grant number RR1693 from the National Institutes of Health, Division of Research Resources. SCoP includes a language for expressing the model in familiar equation form, as well as a library of solvers and an interactive simulation environment. The compiled model was run on a Intel 80486/25 microprocessor based digital computer. The integration algorithm was an adjustable step size modified Euler method. Such an adjustable step size method was required because of the large gradients imposed when the model was subjected to rapid changes in ambient conditions.

The thermoneutral temperature for each node was determined by solving the steady-state equations. This was done with the matrix inversion approach using a commercially available computer spreadsheet program.

RESULTS

Water immersion.

Figure 1 shows the experimental MR data (solid squares and circles) from Hayward et al. (7,8) as compared to the predictions of the model (solid and dashed lines) for water immersion in 0°C and 10°C water, respectively. The data are expressed as multiples of the pre-immersion (basal) MR. As seen, a prominent feature of the experimental data is an initial rapid increase in MR, which is presumed to be due to the rapid decrease in skin temperature upon cold water immersion (see Fig. 3). However, this feature is transient, as the MR falls back to much lower levels over the next few min. At 3-5 min. after immersion, the MR begins to rise again and reaches near maximum values at 10 min. for the 0°C water immersion. In contrast, for the 10°C immersion, the MR plateaus at an intermediate value (3 times basal) until ~30 min, and then rises to near maximum values by 45 min. The model-predicted curves generally mimic the shape of the data; however, the very rapid fall in MR for the 0°C data (squares) after the initial peak occurs a few minutes later in time for the model predictions (solid line) and the plateau in the 10°C data (circles) is only roughly approximated by the model (dashed line). In our attempts to predict these experimental data and the data for higher temperatures presented below, it was clear that inconsistencies in the data must exist; features existed in 1 data set not present in others. Therefore, model predictions did not exactly duplicate any one set, but the overall predictions were good.

To produce the fits shown in Fig. 1, controller parameter values had to be determined. These values are shown in Table 3. The value of the A_{sl} parameter, coupled with the rate of decrease of skin temperature, determined the initial MR peak. However, for the 0°C data, the peak was further limited by the value for S_{lmax}. Figure 2 shows the 3 components of the metabolic response to the 0°C immersion. As seen, the S_l component rises rapidly to a maximum determined by S_{lmax}

TABLE 1

Determination of steady-state component of S_3

T_s	$\frac{dTc}{dt}$	$\frac{dTc}{dt}(T_s - 34)$	ΔMR	
°C	°C/min	(°C/min)·°C	Kcal/hr/m^2	
			Experimental	Predicted[†]
26.7[*]	-0.098	0.715	114	117
28.9	-0.086	0.439	70	72.1
30.7	-0.091	0.300	62	49.3
33.4	-0.0104	0.062	5.5	10.1

T_s, skin temperature; T_c, core temperature; ΔMR, change in metabolic rate from baseline.
[*]Experimental data in Tables 1 and 2 are derived from the data of Nadel and Horvath (12).
The following equation was assumed to predict[†] the MR data with the constant of 164 found to

$$\Delta MR = 164 \frac{dT_c}{dt}(T_s - 34)$$

provide the best fit using linear, least-squares regression analysis (1). This constant was taken as A_{s3} in Eq. 3, T_c is assumed to be equivalent to T_h in that Eq., and the change in T_s from 34°C is equivalent to the integrated *COLDS* signal.

and the limit is sustained for another min, as shown by the arrows. Then the contribution of this component decreases rapidly, and by 10 min, it no longer has a significant role. The magnitude of S_1 is closely coupled to the rate of decrease in skin temperature, as seen in Figure 3. The time-lag term suggested by Wissler (23) was not incorporated in this response because it would have further delayed the reduction of the MR after the initial peak. The very close comparison between experimental skin temperature data and model predictions was produced by increasing by a factor of 14 each of the skin-air heat transfer coefficients upon water immersion. As seen in Figure 3, the first data point for the 0°C immersion case was 5 min after immersion. Therefore, it is possible that the experimental skin cooling rate before 5 min approached steady state faster than the simulation result. If so, this factor could account for the apparent delay in the predicted MR response in Figure 1.

The A_{s2} parameter partially determines the steady-state MR during the immersion, but is also a factor in the transient changes. In Figure 1, this parameter was partially responsible for the steep rise in MR predicted by the model at 5 - 10 min, but thereafter, the limits on S_2 and S_3 had more important effects. At higher water temperatures, these limits did not come into play; therefore, the A_{s2} value was determined primarily to match near steady-state MR data during immersion at these higher water temperatures (see Figure 5). The variable limit on S_2 was determined to modulate the rapid rise in MR after the initial peak, especially for the 10°C data. As seen by the arrows in Figure 2, S_2 is limited for all times >8 min after immersion for the 0°C data and it was limited for all times >12 min for the 10°C data (not shown).

The A_{s3} and K_{s3} parameters were determined from the experimental data of Nadel and Horvath (12) given in Tables 1 and 2. The resulting magnitude of the S_3 component is shown in Figure 2. As seen, it plays the most dominant role in determining longer term MR increases for the 0°C immersion case because the largest changes in the rate of decrease of core temperature and of the decrease in skin temperature occur for this lowest temperature. For the 10°C immersion and higher temperatures, the S_3 term plays a less dominant role than the S_2 term in determining increases in MR. Also seen in Figure 2 is that it was necessary to limit S_3 to ensure that the total MR did not increase beyond the maximum limits shown in Figure 1. From a modelling approach, this effect also could have been achieved from the limit on total MR.

Hypothalamic (head-core) temperature decrease is a primary stimulus for shivering. However, this temperature is not generally measurable, but the related rectal (trunk-core) temperature is usually measured. Figure 4 shows experimental data (solid squares and circles) of Hayward et al. (7,8) for water immersion at 0°C and 10°C temperatures, respectively. As seen, after the initial 5-min period where the temperature change was small, the rectal temperature began to fall rapidly and the rate of decline increased with time for both immersion temperatures. This rapid rate of decline helps to produce the steep increase in the S_3 component seen in Figure 2, and the absolute decrease in temperature also drives the increase in the S_2 component. The model predictions (solid and dashed lines) for these temperature changes were quite good, in general, although the predicted results did not fall as rapidly as the experimental data in the later stages of the immersions.

MR data from the study of Tikuisis et al. (17) are shown in Figure 5 for immersion at 20°C and 28°C temperatures. As seen, these data do not show the initial MR peak, which is very prominent in the Hayward et al. (7) study (see Figure 1). The absence of this feature may be due to the wide spacing of the data points (6 min apart). However, the Tikuisis et al. (17) data also look different because they reach values of near steady-state by the first sample, in contrast to the responses shown in Figure 1. The model predictions are quite close to the experimental data after >20 min of immersion, but they do not show the sustained high values of MR shown early in the experimental data. These differences in MR patterns for the different data sets make it very difficult to accurately predict the data over the whole time range with a single set of constant controller parameters.

Rectal temperature changes measured by Tikuisis et al. (17) are shown in Figure 6. The 28°C immersion data (solid circles) are predicted quite well by the model, but the model grossly overestimates the decrease in rectal temperature for the 20°C immersion case. It appears that the experimental data for both temperatures are very close, even though the MR patterns shown in Figure 5 are distinct. At present, we cannot reconcile this inconsistency; however, it underscores the necessity of comparing model predictions to a number of experimental data sets.

Exposure to cooled air.

To see how well the model predicts thermal behavior in response to a different stress, a comparison was made to the data of Raven and Horvath (14) for exposure to 4.7°C air, as presented by Gordon et al. (4). This data set includes both MR data as well as extensive skin temperature data, which provides a comprehensive test of the model. Figure 7 shows the MR experimental data (solid circles) and the model prediction (solid line). It is clear that the prediction is generally acceptable, considering no controller parameter adjustments were made. Skin temperature data are shown in Figures 8 and 9. As shown, our model underestimates the arm-skin data significantly, whereas the leg data are predicted quite closely. The finger and toe data show a somewhat more rapid approach to steady-state than the model predictions for the hand and foot, but considering the anatomical difference for experimental and predicted results, the comparison is satisfactory. It is likely that altering the partitioning of blood flow and shivering metabolism to these sections would improve the fit. However, since the bodily compositions of the experimental subjects in the various studies were significantly different, we decided not to make changes to the model to make it fit any one data set.

One significant discrepancy observed for the air-cooling data was that the experimentally measured rectal temperature (4) increased by about 1°C during the 2 hrs of exposure. In contrast, the model prediction was a 1°C decrease. At present, we cannot explain this discrepancy. Timbal et al. (19) also found that rectal temperature increased when subjects were exposed to cool air, but they also found that immersion in water down to 24°C produced initial increases in rectal temperature, which contrasts to the data of Tikuisis et al. (17). These differences in experimental data cannot presently be explained.

Cabin water spray system.

The next objective was to use the model to predict thermoregulatory responses after an individual had been wetted by a cabin water spray system and exposed to a cool environment. The basic model had to be modified by adding the effects of clothing and a water layer next to the skin, which evaporates and draws heat from the skin.

The effects of the CWSS were evaluated by determining the spray induced changes in MR, trunk-core temperatures, and various skin temperatures during exposure up to 1 hr to ambient air conditions of temperatures down to 0°C with wind velocities up to 40 MPH. Figure 10 shows the decrease in the mass of the sprayed water layer on the thorax as the layer evaporates. The conditions imposed are 25% body wetting, which is the maximum considered, and 0°C ambient air. The upper line shows that under normal wind conditions the mass of the layer decreases about 40% over the 60-min period after spraying. The rate of decrease is almost constant because it depends only on the vapor pressure of the water layer, which in turn depends upon the water-layer temperature, which changes very little over this period (see Figure 11). When the ambient air temperature was 24°C, the decrease in mass was almost identical. With a 40 MPH wind velocity, the evaporation of the layer is much more rapid because of the increase in the convective heat-transfer coefficient. As seen, the layer completely disappears in <15 min after exposure to the wind.

The temperature of the water layer on the thorax under the various wind conditions is shown in Figure 11. The temperature rises slightly even when the ambient temperature is 0°C because the high conductivity from the skin produces heat transfer to the layer sufficient to overcome the loss to the environment. However, when the wind velocity increases to 40 MPH, the combination of the low ambient temperature and the increased convective heat loss produces a rapid decrease in water-layer temperature which cools the skin. Data from the water layers on the head and arms are similar in their transient behavior.

Table 4 shows changes in selected variables for 60 min of exposure to changes in ambient conditions both for the unsprayed (top section) and sprayed individual. It is clear that the CWSS produces the largest changes under the normal ambient conditions. Core (rectal) and skin temperatures dropped by 0.6 and 3.9°C, respectively, whereas MR increased by 50%. When air temperature was reduced to 0°C (24.1°C decrease), the changes in core and skin temperatures relative to the unsprayed condition were only -0.29 and -1.7°C, respectively. The MR increased from 2.05 times basal to 2.61 times after spraying. For the high wind velocity condition, spraying produced very little further decreases in temperatures or increase in MR over the effect of the high velocity itself. Therefore, the CWSS would not appear to significantly increase the risk of exposure to a harsh environment.

DISCUSSION

The purpose of this study was to develop a mathematical model of human temperature regulation under cold conditions that could be used to predict the thermal response to a cabin

water spray system activated during a fire. Since the individual would be wet on parts of the body and then could be exposed to very cold and windy conditions upon exiting the airplane, it was necessary for the model to accurately simulate conditions similar to cold-water immersion over a range of water temperatures.

We used the classic 25-node model of Stolwijk and Hardy (16) with parameters modified anatomically by Tikuisis et al. (18) with the general 3-component approach of Wissler (23) for the shivering controller. This model could predict with reasonable accuracy transient data for metabolic rate, rectal and skin temperature after cold-water immersion (see Figures 1 and 3-6). Therefore, it is highly likely that it can predict, with sufficient accuracy, the response to skin wetting by the CWSS. The major finding was that compared to the effects of cold-air and high-wind exposure, the effect of the CWSS was relatively small (see Table 4). The greatest stress to the human thermal system was seen under normal environmental conditions, but even here, the effect was not large.

There is still considerable argument over both the anatomical description (i.e., number of nodes) and the form of the controller equations to describe human thermal responses to cold conditions. Whereas these arguments are unlikely to influence our conclusion that the CWSS would have insignificant effects on airline passengers, it is important for other applications that they be resolved.

The question of the number of nodes required has been directly addressed only in 1 situation. Wissler (21) compared responses of head-core and trunk-skin temperatures in his 250-node model and the 14-node model of Kuznetz (10) to a combination of air cooling and light exercise. The important finding was that the 14-node model significantly overestimated the decrease in skin temperature. Wissler suggested that any time thermal gradients between core and skin are significant, these errors would occur. There are no similar studies to evaluate the decrease in this error of expanding the model to 25-nodes, or even larger, as did Gordon et al. (4) and Montgomery (11). In the case of water immersion, the overestimation in the skin temperature would probably be decreased because of the rapid equilibration between skin and water temperatures, but the resulting large gradient between skin and core might produce similarly large errors in the core temperatures.

The form of the controller equations for shivering is still not settled. The original model of Stolwijk and Hardy (15) postulated that the increase in MR was dependent on the product of changes in average skin temperature and the head-core temperature. This assumption was not altered in their subsequent model (16) or in the changes made by Montgomery (11) to adapt the model for water immersion predictions. Gordon et al. (4) made the first substantial change. They assumed that the MR increase was sensitive to a sum of three terms, each proportional to either 1) skin temperature, 2) head-core temperature, or 3) heat flux. They found controller parameter values that produced close prediction of transient MR, rectal temperature, and various skin temperatures during exposure to ~5°C air. However, Wissler (21) found that this model was unable to predict the thermal response to cold-water immersion.

In 1985, Wissler (23) suggested a different 3-component shivering MR controller. The MR was a sum of terms proportional to 1) the time-rate of change of mean skin temperature (dT_s / dt), 2) the product of the changes in mean skin temperature and central (core) temperature as formulated by Hayward et al. (8), and 3) the time-rate of change of central temperature. Wissler formulated the first component (S_1) as a set of differential equations, each governing the change in MR at different magnitudes of dT_s / dt. However, he gave little justification for his assumptions, nor did he list most of the parameter values required to use this formulation. There is substantial evidence that there is a rapid transient increase in MR coincident with a drop in skin temperature. This response is very evident in the data of Hayward et al. (7,8) during cold-water immersion, in the data of Raven and Horvath (14) during cold-air exposure, and in the results of Timbal et al. (19) for both cold-water immersion and cold-air exposure. Consequently, we incorporated this effect in the present model, but we found that to fit the available MR data, it was not necessary to describe it by a set of differential equations. Instead, as given by Eq. 1, the S_1 component was simply proportional to the sum of the weighted rates of change of the individual skin temperatures. The time lags introduced by the differential equations would have slowed the MR increase upon cooling, which was not indicated by the experimental data (see Figure 1). In contrast, Tikuisis et al. (17) did not incorporate this effect in their model. Instead, they had a term proportional to skin temperature, which they included to produce a rapid increase in MR with skin cooling because their experimental MR data (see Figure 5) did not show the subsequent rapid fall in MR as in the data for colder water temperatures (see Figure 1). Perhaps it takes a certain minimum rate of skin temperature decrease to initiate the transient effect, or the effect was not seen in the Tikuisis et al. data because data sampling was not sufficiently rapid.

The second component (S_2) proposed by Wissler (23) was taken from the findings of Hayward et al. (8) during water immersion at 10°C. They proposed that the steady-state MR increase observed could be described by a product relationship of changes in skin and core temperatures. However, the changes were not relative to normal values of these variables, but to reference values of 41 to 42°C, presumably the values at which neural firing from the receptors ceases. It is possible that this relationship is incorrect because Hayward et al. ignored the involvement of time-varying core temperature changes during their measurements. In 1969, Nadel and Horvath (12) showed that a centrally imposed heat debt resulting in a sustained decrease in core temperature of ~0.1°C/min induced a rapid increase in MR peaking at a value dependent upon mean skin temperature, which was held constant at different values during the MR measurements. At the normal skin temperature, the heat debt had no significant effect on the MR. In a subsequent paper, Nadel et al. (13) discussed the presence of a rate component in MR increases, but they did not formalize this component, as they tried to predict only steady-state changes. Wissler (23) recognized that this rate effect could be important and proposed that the third component of shivering (S_3) was proportional to dT_c / dt, but he ignored the modulating effect of skin temperature in this formulation. Assuming the existence of this effect, then the MR data of Hayward et al. (7,8) must have been affected because core temperature was decreasing throughout the measurement period. As a consequence, their expression derived for MR changes is not valid.

single set of controller equations developed in the present study is a step forward, in that one does not have to postulate different equations for different conditions, but the direction of core temperature changes is still unresolved.

TABLE 1

Determination of steady-state component of S_3

T_s	$\frac{dTc}{dt}$	$\frac{dTc}{dt}(T_s - 34)$	ΔMR	
°C	°C/min	(°C/min)·°C	Kcal/hr/m^2	
			Experimental	Predicted†
26.7*	-0.098	0.715	114	117
28.9	-0.086	0.439	70	72.1
30.7	-0.091	0.300	62	49.3
33.4	-0.0104	0.062	5.5	10.1

T_s, skin temperature; T_c, core temperature; ΔMR, change in metabolic rate from baseline.
*Experimental data in Tables 1 and 2 are derived from the data of Nadel and Horvath (12).
The following equation was assumed to predict† the MR data with the constant of 164 found to

$$\Delta MR = 164 \frac{dT_c}{dt}(T_s - 34)$$

provide the best fit using linear, least-squares regression analysis (1). This constant was taken as A_{s3} in Eq. 3, T_c is assumed to be equivalent to T_h in that Eq., and the change in T_s from 34°C is equivalent to the integrated *COLDS* signal.

TABLE 2

Determination of exponential decay rate of S_3

TIME	MR				
Hrs	Fraction of maximum value			Mean ± SE	Predicted†
0.083	0.380	0.640	0.742	0.59 ± 0.11	0.57
0.208	0.200	0.029	0.338	0.19 ± 0.09	0.24
0.542	0.070	0.114	0.226	0.14 ± 0.05	0.02

†Predicted from the equation

$$MR_f = e^{-K_{s3}\, t}$$

where MR_f is the fraction of the maximum MR and the value, $K_{s3} = 6.87$/hr, was found to give the best fit to the mean data.

TABLE 3

Shivering-controller parameter values

PARAMETER	VALUE	UNITS
A_{s1}	0.62	$Kcal \cdot hr^{-1} \cdot (m^2)^{-1}$
A_{s2}	5.67	$Kcal \cdot hr^{-1} \cdot (m^2)^{-1}$
A_{s3}	2.74	$Kcal \cdot hr^{-1} \cdot (m^2)^{-1}$
K_{s3}	6.87	hr^{-1}
S_{1max}	129	$Kcal \cdot hr^{-1} \cdot (m^2)^{-1}$
S_{2max}	Variable (25.8 - 124)†	$Kcal \cdot hr^{-1} \cdot (m^2)^{-1}$
S_{3max}	82.5	$Kcal \cdot hr^{-1} \cdot (m^2)^{-1}$
S_{max}	144	$Kcal \cdot hr^{-1} \cdot (m^2)^{-1}$

†This limit varied exponentially with time with a time constant of 0.8 hrs.

TABLE 4

Thermal response to CWSS

	TEMPERATURE CHANGE (°C)			
WIND VELOCITY	AIR	CORE	SKIN	METABOLIC RATE
MPH				x BASAL
UNSPRAYED				
0.22	0	0	0	1.00
0.22	-24.1	-0.69	-7.1	2.05
40	0	-0.61	-5.7	1.70
40	-24.1	-2.15	-21.1	4.53
SPRAYED				
0.22	0	-0.60	-3.9	1.50
0.22	-24.1	-0.98	-8.8	2.61
40	0	-0.65	-5.7	1.73
40	-24.1	-2.17	-21.1	4.53

REFERENCES

1. Daniel, W.W. *Biostatistics: A Foundation for Analysis in the Health Sciences*, New York:Wiley, 1987. Ed. 4

2. Gagge, A.P., A.P. Fobelets and L.G. Berglund. A standard predictive index of human response to the thermal environment. *ASHRAE Trans.* 92:709-731, 1986.

3. Gagge, A.P. and Y. Nishi. Heat exchange between human skin surface and thermal environment. In: *Handbook of Physiology. Adaptation to the environment*, edited by Lee, D.H.K. Bethesda: Am. Physiol. Soc., 1964, p. 69-92.

4. Gordon, R.G., R.B. Roemer and S.M. Horvath. A mathematical model of the human temperature regulatory system - Transient cold exposure response. *IEEE Trans.Biomed.Eng.* BME-23:434-444, 1976.

5. Hardy, J.D. Models of temperature regulation - a review. In: *Essays on Temperature Regulation*, Amsterdam: North-Holland, 1972, p. 163-186.

6. Haslam, R.A. and K.C. Parsons. Using computer-based models for predicting human thermal responses to hot and cold environments. *Ergonomics* 37:399-416, 1994.

7. Hayward, J.S. and J.D. Eckerson. Phsiological Responses and survival time prediction for humans in ice-water. *Aviat.Space Environ.Med.* 55:206-212, 1984.

8. Hayward, J.S., J.D. Eckerson and M.L. Collis. Thermoregulatory heat production in man: prediction equation based on skin and core temperatures. *J.Appl.Physiol.* 42:377-384, 1977.

9. Holman, J.P. *Heat Transfer*, New York:McGraw-Hill, 1968. Ed. 2

10. Kuznetz, L.H. A model for the transient metabolic thermal response of man in space. *NASA Manned Spacecraft Center Internal Note* MSC-Ec-R-68-4:1966.

11. Montgomery, L.D. A model of heat transfer in immersed man. *Ann.Biomed.Eng.* 2:19-46, 1974.

12. Nadel, E.R. and S.M. Horvath. Peripheral Involvement in thermoregulatory response to an imposed heat debt in man. *J.Appl.Physiol.* 27:484-488, 1969.

13. Nadel, E.R., S.M. Horvath, C.A. Dawson and A. Tucker. Sensitivity to central and peripheral thermal stimulation in man. *J.Appl.Physiol.* 29:603-609, 1970.

14. Raven, P.R, and S.M. Horvath. Variability of physiological parameters of unacclimatized males during a two-hour cold stress, 5∘C. *Int.J.Biometeorol.* 14:309-320, 1970.

15. Stolwijk, J.A.J. and J.D. Hardy. Temperature regulation in man - A theoretical study. *Pflugers Arch.* 291:129-162, 1966.

16. Stolwijk, J.A.J. and J.D. Hardy. Control of body temperature. In: *Handbook of physiology. Reaction to environmental agents*, edited by Lee, D.H.K. Bethesda: Am. Physiol. Soc., 1977, p. 45-67.

17. Tikuisis, P., R.R. Gonzales and K.B. Pandolf. Thermoregulatory model for immersion of humans in cold water. *J.Appl.Physiol.* 64:719-727, 1988.

18. Tikuisis, P., R.R. Gonzales and K.P. Pandolf. Human thermoregulatory model for whole body immersion in water at 20 and 28∘C. *US Army Res.Inst.Env.Med.* T23-87:1-46, 1987.

19. Timbal, J., C. Boutelier, M. Loncle and L. Bogues. Comparison of shivering in man exposed to cold in water and air. *Pflugers Arch.* 365:243-248, 1976.

20. Wissler, E.H. A mathematical model of the human thermal system. *Bull.Math.Biophys.* 26:147-166, 1964.

21. Wissler, E.H. Comparison of computed results obtained from two mathematical models - A simple 14-node model and a complex 250-node model. *J.Physiol.Paris* 63:455-458, 1971.

22. Wissler, E.H. An Evaluation of Human Thermal Models. Part A. *US Air Force. (Sci. Res. Rep. AFOSR-82-0214)* 1984.

23. Wissler, E.H. Mathematical simulation of human thermal behavior using whole body models. In: *Heat transfer in medicine and biology*, edited by Shitzer, A. and Eberhart, R.C. New York: Plenum, 1985, p. 325-373.

ACKNOWLEDGEMENTS

We would like to thank the Federal Aviation Administration's Technical Center for their support of this project.

FIGURE LEGENDS

1. Change in metabolic rate relative to basal level after immersion in cold water. The filled squares and circles are experimental data from Hayward et al. (7,8) at 0 and 10°C, respectively, whereas the solid and dashed lines represent the corresponding model predictions.

2. Predicted increases in metabolic rate induced by the 3 components of the shivering controller for a 0°C water immersion. The time intervals between the arrows are the times for which the components had reached the maximum value allowed.

3. Experimental data (7,8) and model predictions of mean skin temperature changes after immersion.

4. Experimental data (7,8) and model predictions (trunk-core temperature) of rectal temperature changes after immersion.

5. Change in metabolic rate relative to basal level after immersion in cool water. The filled squares and circles are experimental data from Tikuisis et al. (17) at 20 and 28°C, respectively, whereas the solid and dashed lines represent the corresponding model predictions.

6. Experimental data (17) and model predictions (trunk-core temperature) of rectal temperature changes after immersion.

7. Comparison between experimental data from Gordon et al. (4) and model predictions of increases in metabolic rate due to exposure to cold air. The shivering-controller parameter values were unchanged from the water-immersion conditions.

8. Comparison between experimental data (4) and model predictions for various skin temperatures during cold-air exposure.

9. Comparison between experimental data (4) and model predictions for various skin temperatures during cold-air exposure.

10. Model-predicted changes in the mass of water on the thorax after the subject was sprayed and then subjected to cold and windy environmental conditions.

11. Temperature changes of the water layer for the conditions shown in Fig. 10.

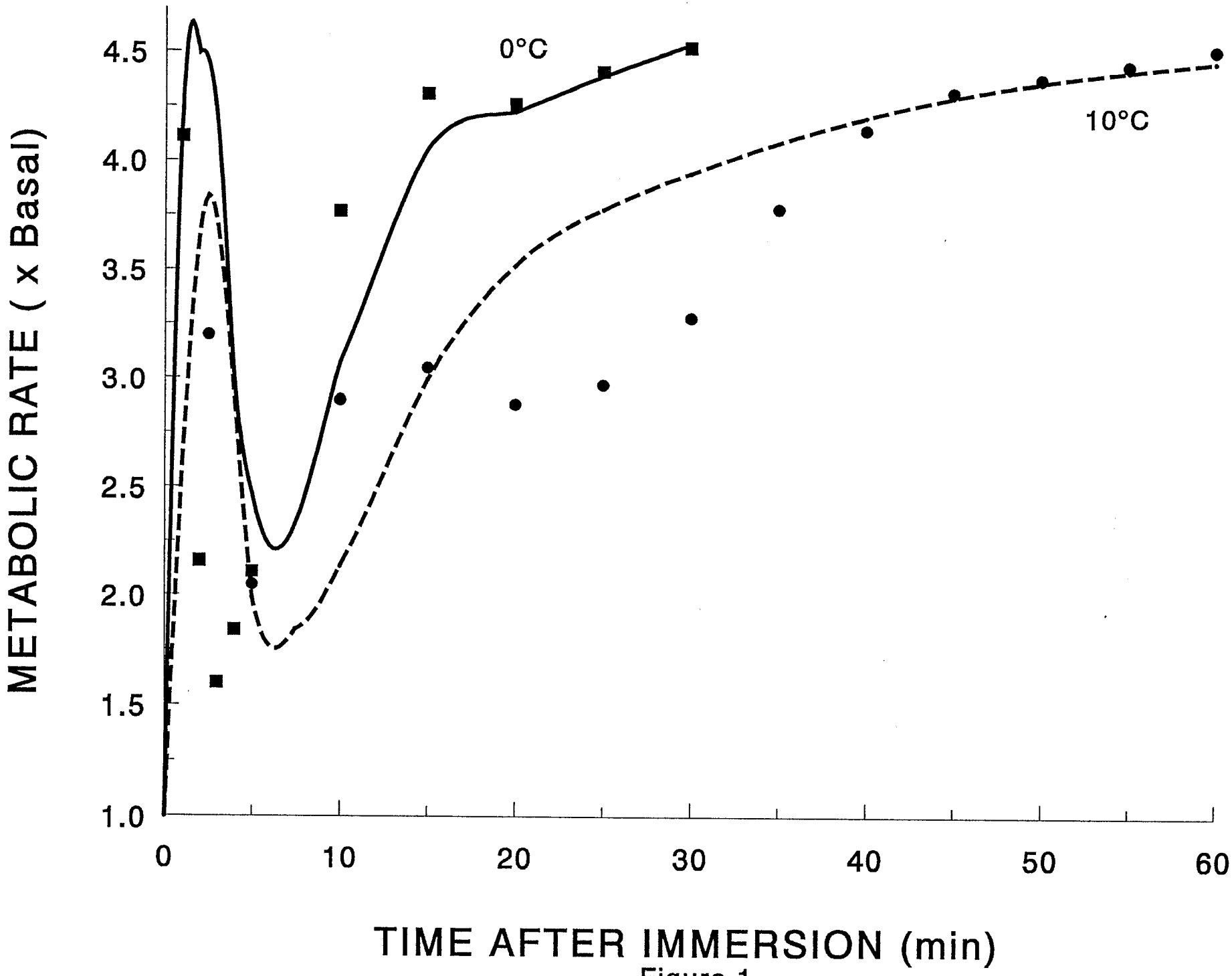
METABOLIC RATE (x Basal)
4.5
4.0
3.5
3.0
2.5
2.0
1.5
1.0
0°C
10°C
0
10
20
30
40
50
60
TIME AFTER IMMERSION (min)

Figure 1

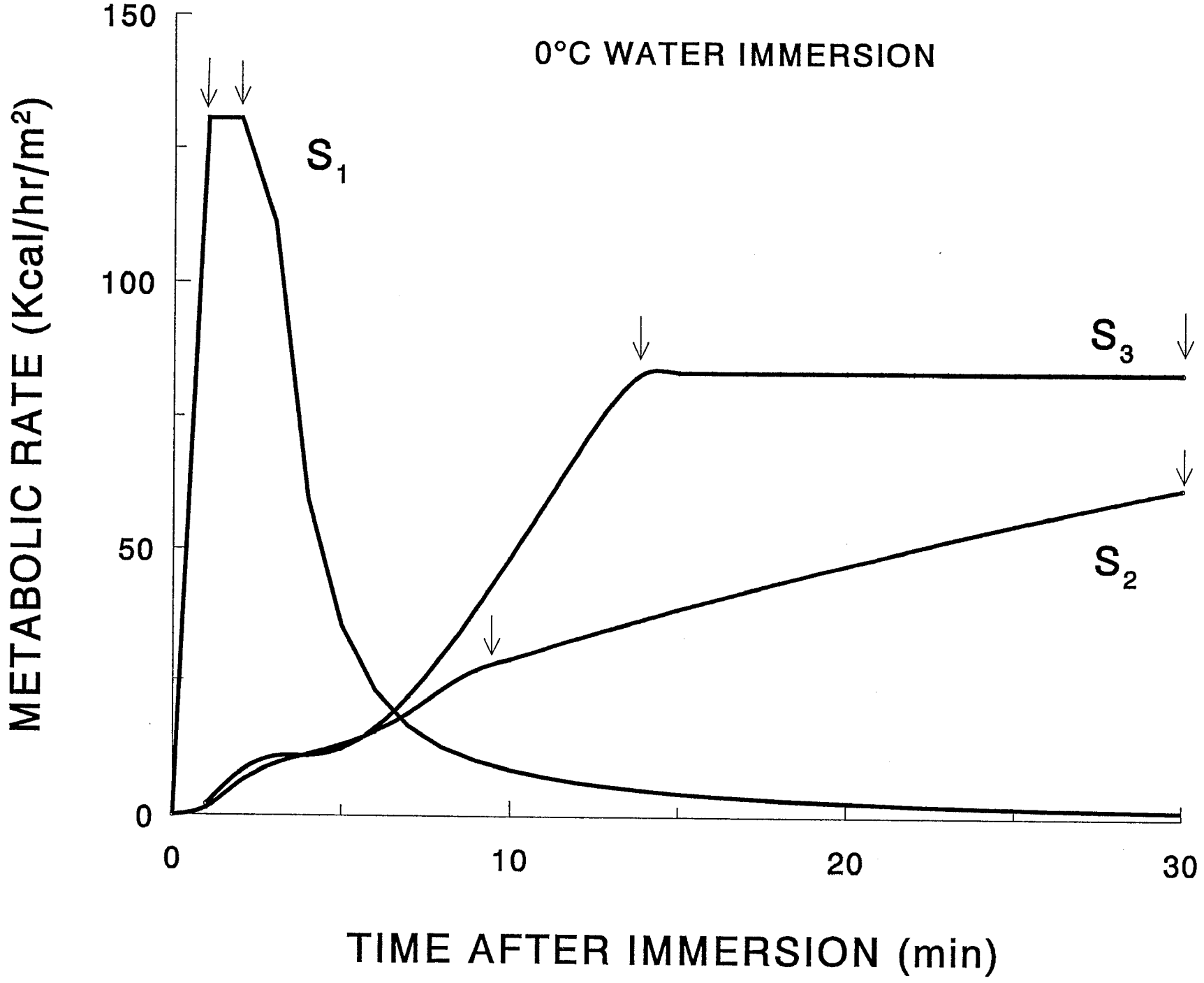
0°C WATER IMMERSION
METABOLIC RATE (Kcal/hr/m²)
150
100
50
0
S1
S2
S3
0
10
20
30
TIME AFTER IMMERSION (min)

Figure 2

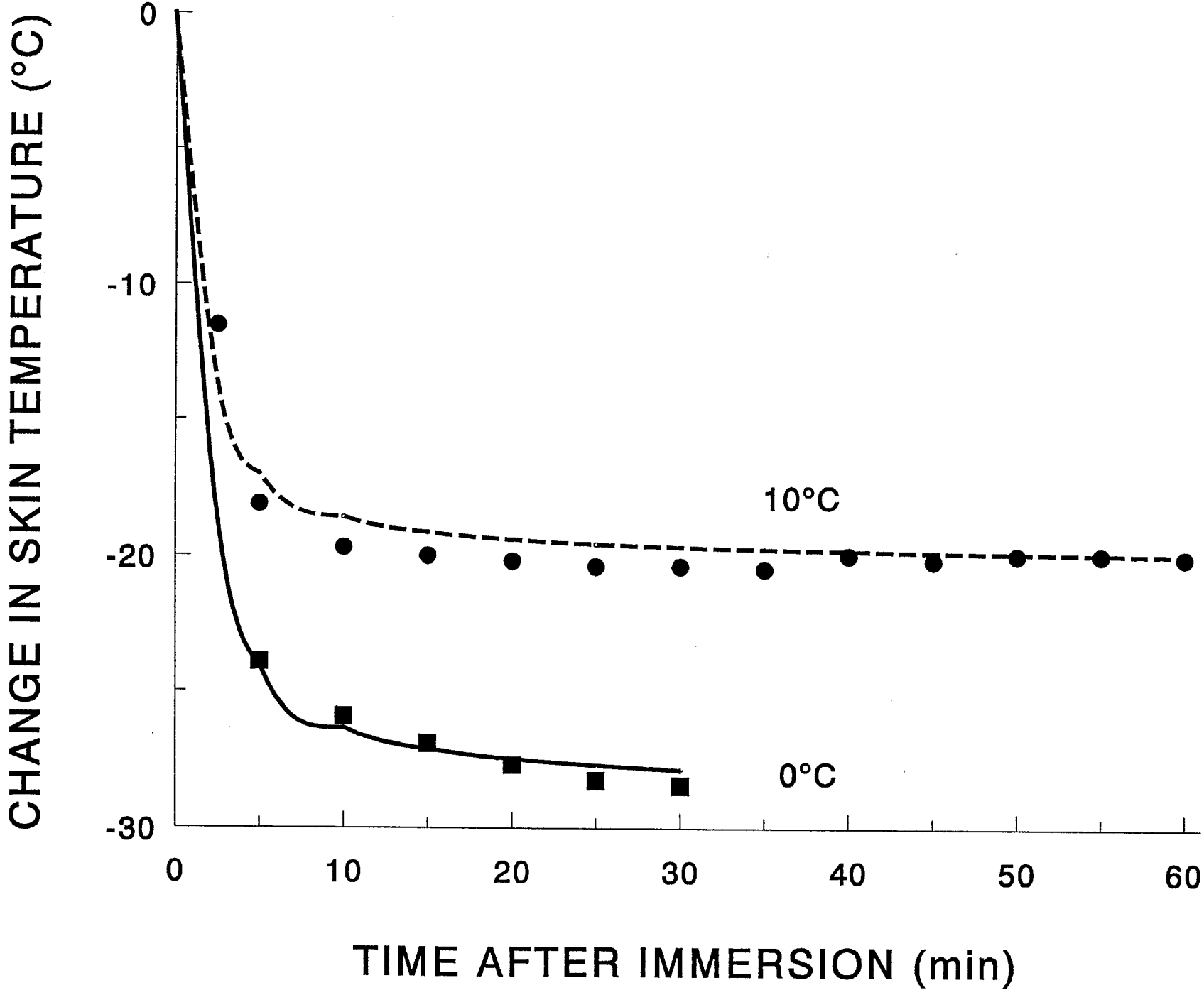
CHANGE IN SKIN TEMPERATURE (°C)
0
-10
-20
-30
10°C
0°C
0
10
20
30
40
50
60
TIME AFTER IMMERSION (min)

Figure 3

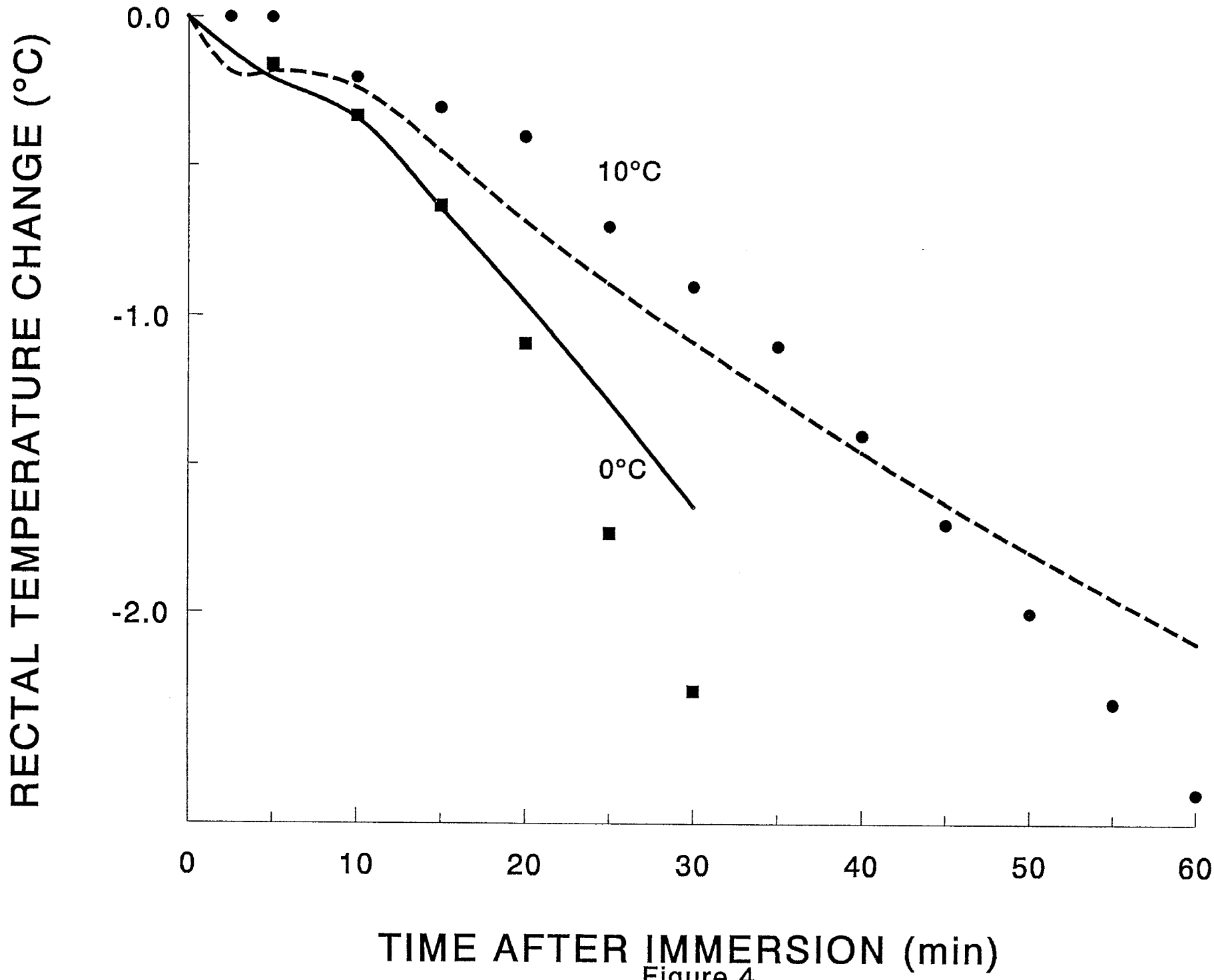
RECTAL TEMPERATURE CHANGE (°C)
0.0
-1.0
-2.0
10°C
0°C
0
10
20
30
40
50
60
TIME AFTER IMMERSION (min)
Figure 4

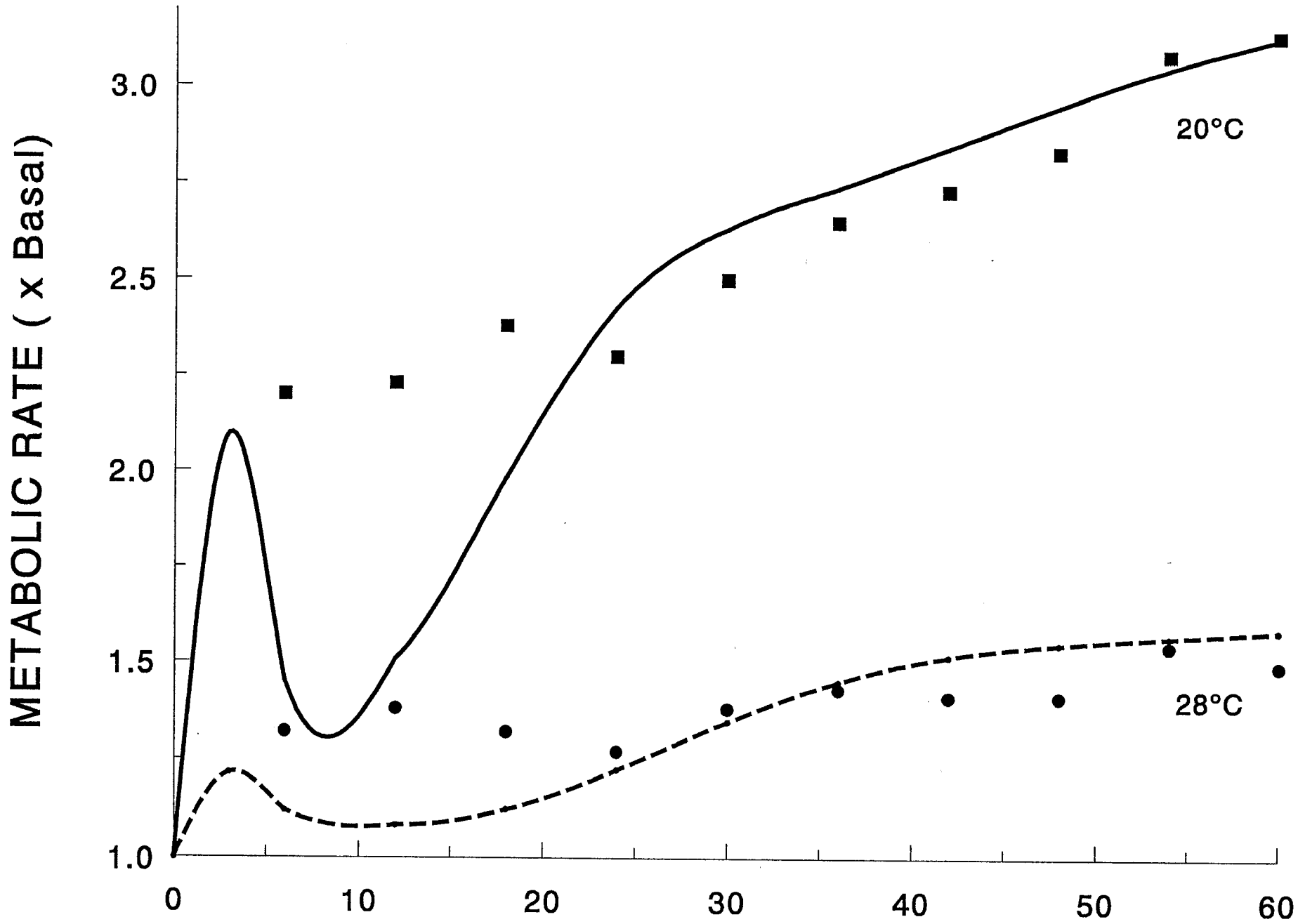
METABOLIC RATE (x Basal)
3.0
2.5
2.0
1.5
1.0
20°C
28°C
0
10
20
30
40
50
60
TIKU1-1b (7/15/94)
TIME AFTER IMMERSION (min)

Figure 5

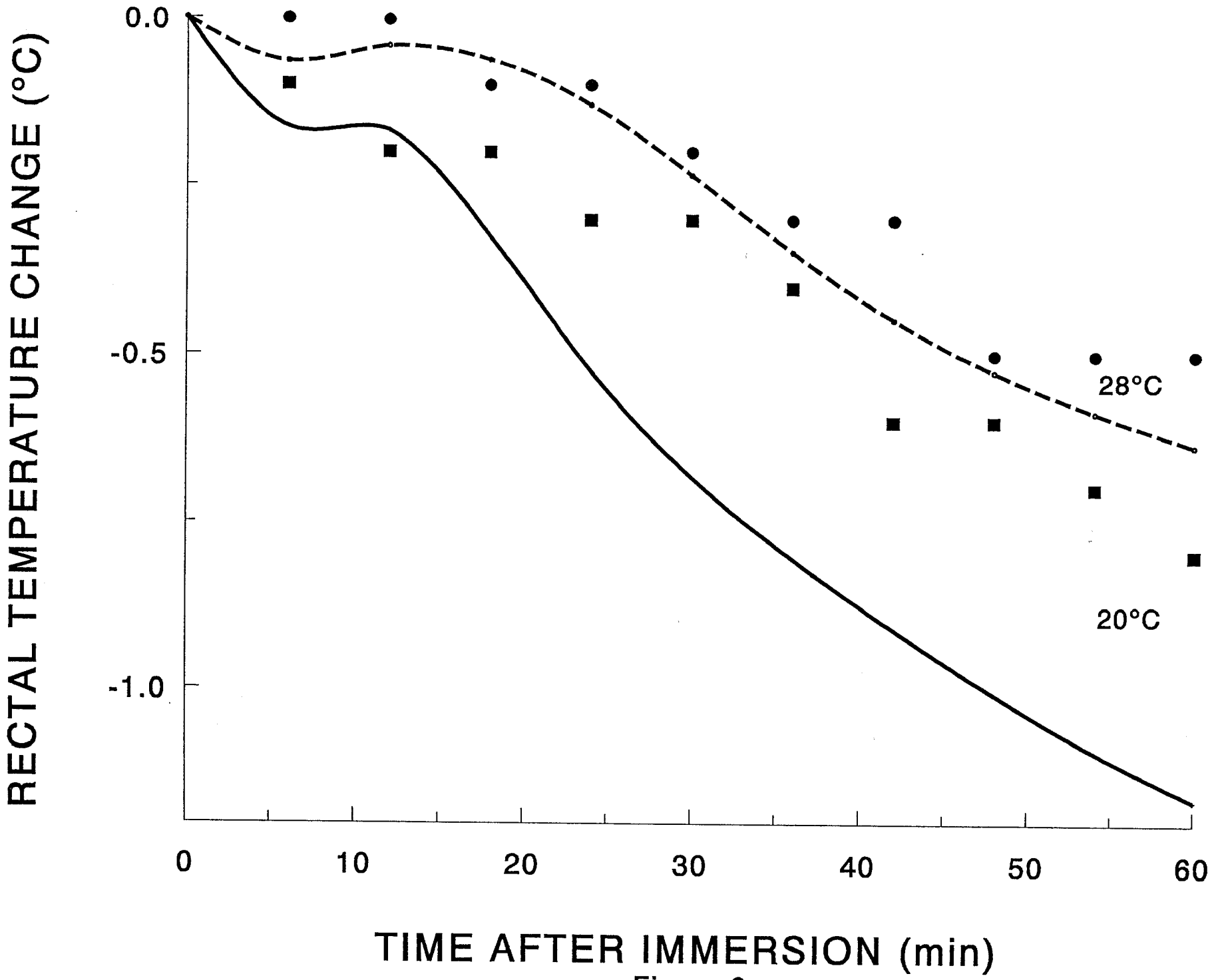
RECTAL TEMPERATURE CHANGE (°C)
0.0
-0.5
-1.0
28°C
20°C
0
10
20
30
40
50
60
TIME AFTER IMMERSION (min)

Figure 6

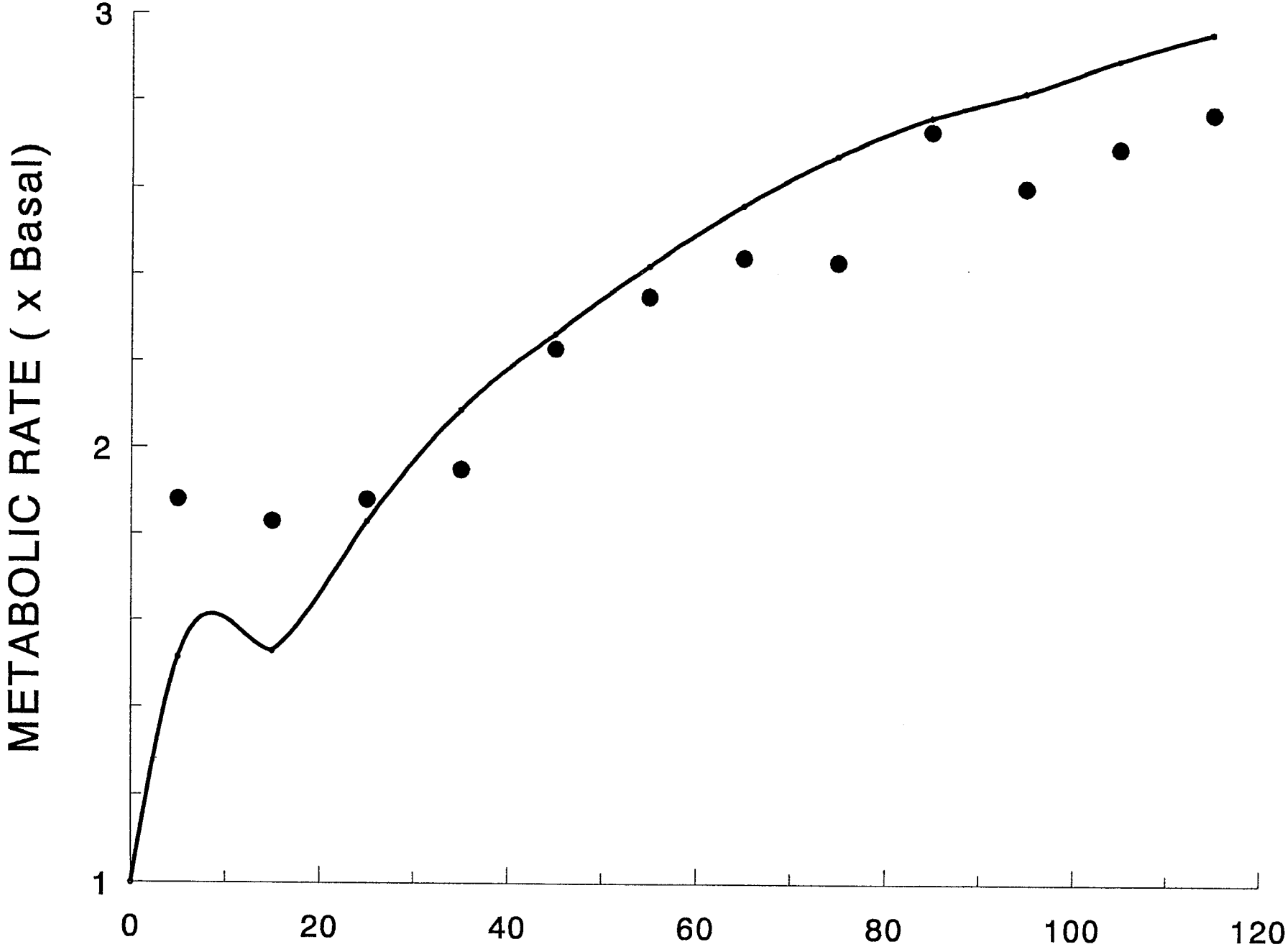
METABOLIC RATE (x Basal)
3
2
1
0
20
40
60
80
100
120
TIME AFTER EXPOSURE TO 4.7°C AIR (min)

Figure 7

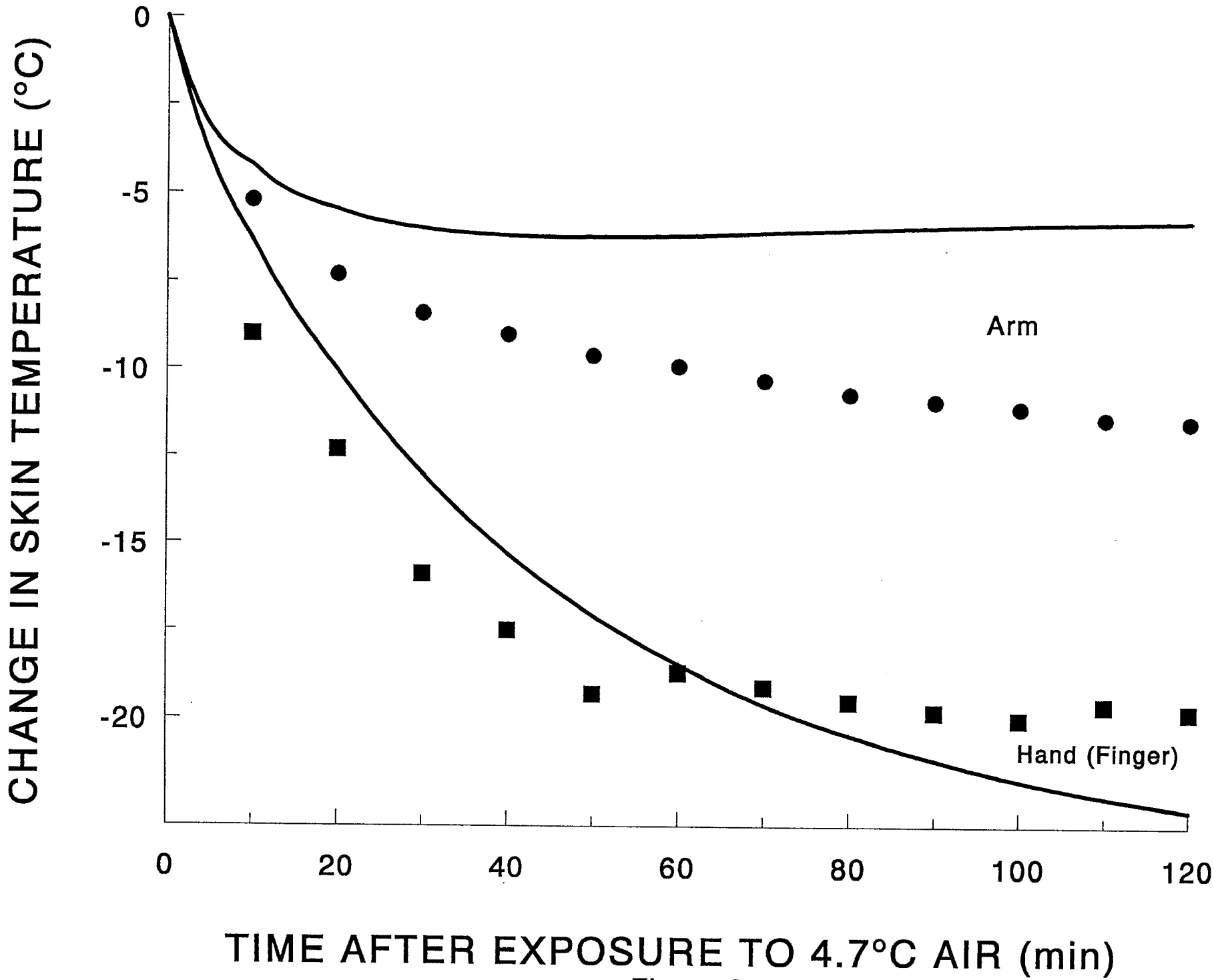
CHANGE IN SKIN TEMPERATURE (°C)
0
-5
-10
-15
-20
Arm
Hand (Finger)
0
20
40
60
80
100
120
TIME AFTER EXPOSURE TO 4.7°C AIR (min)

Figure 8

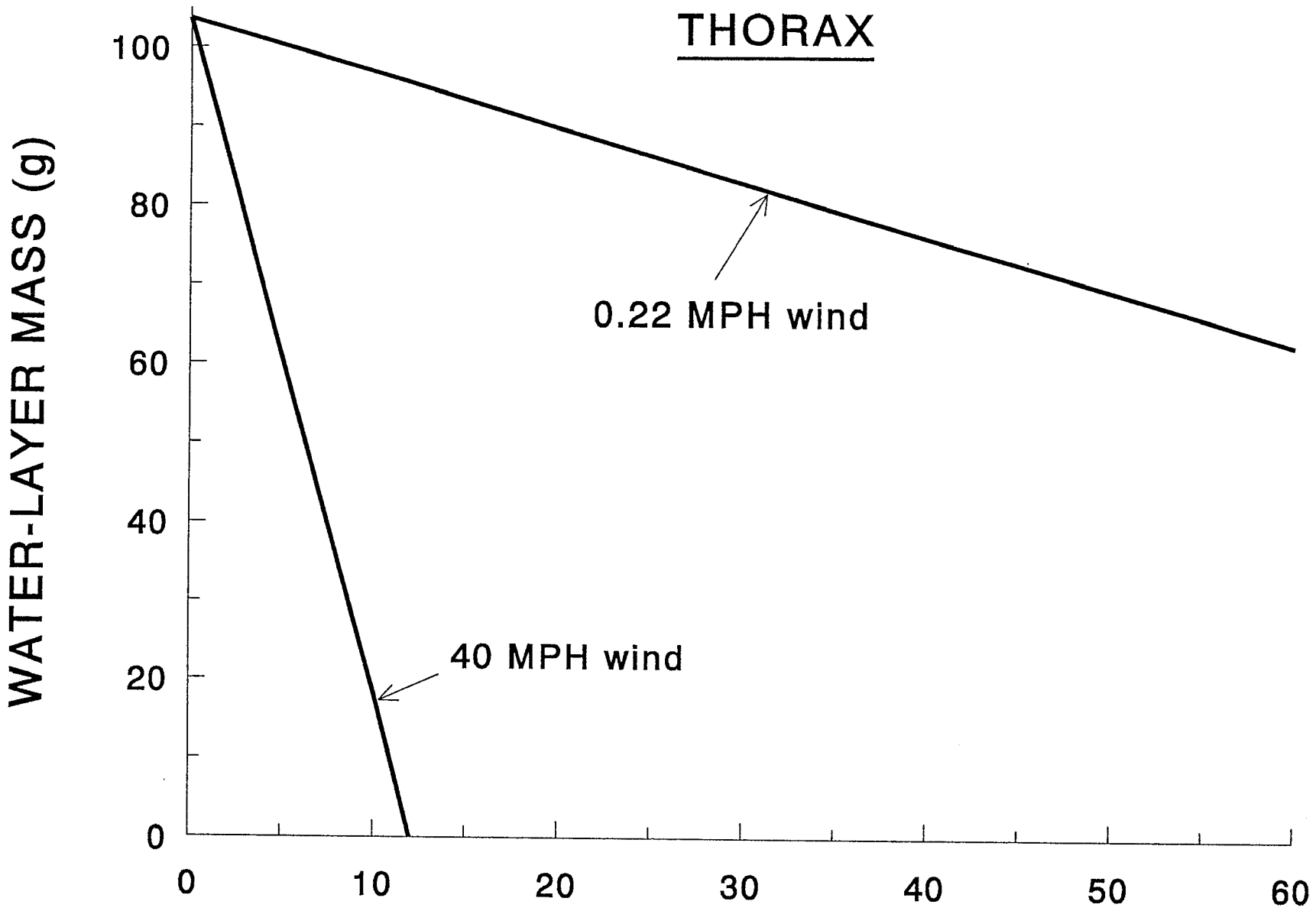
THORAX
WATER-LAYER MASS (g)
100
80
60
40
20
0
0.22 MPH wind
40 MPH wind
0
10
20
30
40
50
60
TIME AFTER SPRAYING (min)

Figure 10

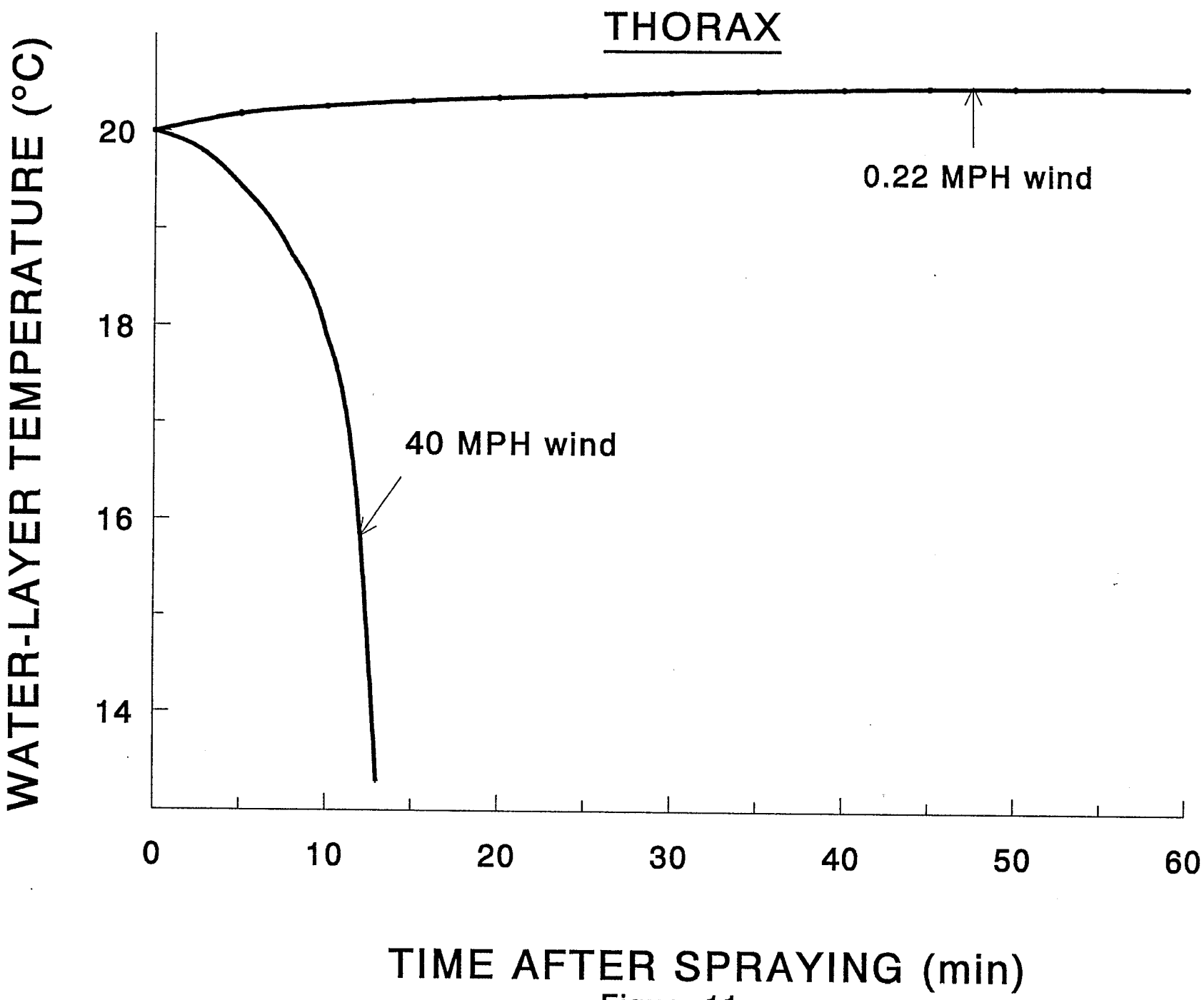
THORAX
WATER-LAYER TEMPERATURE (°C)
20
18
16
14
0.22 MPH wind
40 MPH wind
0
10
20
30
40
50
60
TIME AFTER SPRAYING (min)

Figure 11